JOURNAL OF GEOPHYSICAL RESEARCH, VOL. 99, NO. B5, PAGES 9025–9033, MAY 10, 1994

Theory of partial thermoremanent magnetization in multidomain grains 2. Effect of microcoercivity distribution and comparison with experiment

Song Xu and David J. Dunlop

Geophysics Laboratory, Department of Physics, University of Toronto, Toronto, Canada

We extend the thermoremanent magnetization (TRM) and pTRM theories developed in paper 1 (Dunlop and Xu, this issue) to grains in which domain walls are pinned by microcoercivities of varying magnitudes. Assuming microcoercivities to be exponentially distributed, we find that the intensity of a total TRM is linearly proportional to the inducing field H_o for small H_o, to a power of roughly $1-1/n$ for intermediate H_o, and independent of H_o for large H_o, similar to the results obtained in paper 1. Here n represents the temperature dependence of microcoercivity that goes as the n th power of the saturation magnetization $M_s(T)$. The above three field dependent regions correspond to thermally blocked, field-blocked and reequilibrated walls, respectively. When being thermally demagnetized, a TRM induced in a high field has low unblocking temperatures, as observed. For a partial TRM acquired from T_2 ($< T_c$) to T_1, there may be no region in which walls are field blocked if the interval (T_2, T_1) is not large enough. This will be the case for magnetite when $T_2 < 565$°C if $n = 2$ or < 500°C if $n = 4$ for $T_1 = T_o$, independent of H_o. If $T_1 > T_o$, an even higher T_2 is required. In such cases, the room temperature intensity of pTRM is approximately proportional to H_o^2 when H_o is small. The resulting thermal demagnetization curve, normalized to the intensity before heating, is independent of both H_o and the mean value of microcoercivities. Complete demagnetization will not occur at a demagnetizing temperature T_2 but only at a temperature close to T_c. The theory is supported by experimental data of thermal demagnetizations of pTRMs measured for various multidomain magnetite samples.

1. Introduction

Dunlop and Xu [this issue] (hereinafter referred to as paper 1) extended Néel's theory of thermoremanent magnetization (TRM) in multidomain (MD) grains to include the acquisition of partial TRM and the thermal demagnetization of total and partial TRM. We assumed that domain walls are pinned by a series of identical and symmetrical energy barriers which result in a single value of microcoercivity h_c. The same assumption was made in all previous TRM theories as well [*Néel*, 1955; *Stacey*, 1958; *Everitt*, 1962; *Schmidt*, 1973; *Dunlop and Waddington*, 1975]. In this paper, we will extend the TRM and partial TRM theories to MD grains having a distribution of microcoercivities. This is necessary for the following reasons.

Unlike single-domain (SD) grains for which a blocking or unblocking temperature spectrum corresponds directly to the distribution of energy barriers, unblocking temperatures of a thermal remanence observed for MD grains result from two mixed effects: one due to continuous reequilibrations of walls through a series of Barkhousen jumps toward a demagnetized state as discussed in paper 1, and the other due to a distribution of microcoercivities. We need a theory that takes both effects into account in order to explain observed thermal demagnetization curves.

We showed in paper 1 that various blocking processes may be involved, particularly during the acquisition of a partial TRM (acquired from $T_2 < T_c$ to T_1). Which particular blocking process is operating in a given pTRM is dependent on the magnitude of h_c relative to the inducing field H_o, as well as on the temperature interval (T_2, T_1). In real grains having a distribution of h_c values, however, various blocking processes can occur at the same time for different walls/grains. Therefore we shall take this distribution effect into account in order to give a coherent picture of how a total or partial TRM is acquired and thermally demagnetized.

Microcoercivity is a microscopic parameter and thus not directly measurable. In the theory developed in this paper, the dependences on h_c values of a partial or total TRM will be reduced to dependences on the mean value of the spectrum of h_c values, which can be related to bulk coercivity using the theory developed by *Xu and Merrill* [1990*a*]. Thus we are able to reduce the uncertainty of the theory when comparing with the experiment.

We will use the same set of symbols as listed in paper 1. However, note that in this paper small h_c and m will be used to denote microcoercivity and magnetization associated with displacements of individual walls, while capital H_c and M will denote the mean values of the distributions of h_c and m values, respectively, for an ensemble of walls/grains.

2. Microcoercivity Distribution in MD Grains

Microcoercivity is defined as the critical internal magnetic field required to unpin a wall trapped by crystal defects [e.g., *Xu and Merrill*, 1989]. In paper 1, we assumed that energy barriers produced by defects that pin walls are identical and symmetrical. This results in a single value of microcoercivity. The assumption is useful in gaining an understanding of the various blocking processes occurring in TRM acquisition. In real grains, however, there exist various types and configurations of defects, resulting in

Paper number 93JB02571.
0148-0227/94/93JB-02571$05.00

irregular energy barriers and thus a distribution of microcoercivities. Such a distribution is conveniently described by a statistical distribution function $f(h_c)$ (the product $f(h_c)dh_c$ is the frequency of occurrence of microcoercivities ranging from h_c to $h_c + dh_c$). For a very large number of randomly distributed defects in individual MD grains, *Xu and Merrill* [1989] showed that $f(h_c)$ is a normal distribution. Experimentally, the distribution of microcoercivities for an MD sample is often revealed by the shape of an alternating field (AF) demagnetization curve [e.g., *Bailey and Dunlop*, 1983]. By subtracting the demagnetizing field from an AF demagnetization curve, *Dunlop* [1983] showed that microcoercivities in most MD rock samples are approximately exponentially distributed. In the present study we assume the distribution function f to be

$$f(h_c) = \frac{1}{H_c} e^{-h_c/H_c}. \tag{1}$$

Xu and Merrill [1990*a*] have shown that the mean value H_c of microcoercivities is well approximated by the measured bulk coercivity for grains each containing a large number of defects.

The temperature variation of h_c values in (1) is taken to follow $M_s^n(T)$, as in paper 1, where n is a constant independent of temperature. An implicit assumption here is that there is only one type of defect operating in MD grains, so that h_c values may vary with position within a grain (determined by local distributions of defects), but they all have the same temperature dependence. This leads naturally to the conclusion that $H_c(T)$ in (1) should be also proportional to $M_s^n(T)$. However, when several types of defects are important, different fractions of h_c values associated with different types of defects may have different temperature dependences [e.g., *Tucker and O'Reilly*, 1980]. In such cases, the temperature variation of the mean microcoercivity H_c represents some average over $h_c(T)$ values. The experimental evidence and its implications will be discussed in later sections.

For a given distribution function $f(h_c)$, the mean magnetization M is determined from

$$M = \int m(h_c) f(h_c)\, dh_c, \tag{2}$$

where the integral should be carried out over the fraction of microcoercivities that are activated in a given magnetization process. In (2), $m(h_c)$ is the magnetization associated with the displacement of an individual wall pinned by a microcoercivity h_c. One complication in determining M from (2) is the fact that magnetizations associated with different walls in a MD grain are magnetostatically coupled. As a result, we have to solve a set of integral equations corresponding to different walls in a grain. This is possible only in certain limited cases [e.g., *Xu and Dunlop*, 1993]. For simplicity, we will use in this paper a noninteracting wall model in which displacements of individual walls in a grain are assumed to be magnetostatically independent of each other. But microcoercivities associated with different walls vary according to the distribution function $f(h_c)$. Strictly speaking, this is a two-domain grain model. A major advantage with the model is that M can be calculated from a single integral equation given by (2). It also allows us to substitute $m(h_c)$ derived in paper 1 directly into (2) for various thermal magnetization processes. A major disadvantage is that we will not be able to consider such effects as magnetic screening of hard remanence by soft or loosely pinned walls, which is a direct result of the mutual-magnetostatic interaction among walls in a grain [*Moon and Merrill*, 1986]. As we will see in the next section, the simplifying assumption of no interaction between walls does lead to some inconsistencies between theory and experiment.

3. INDUCTION OF TOTAL TRM

Following paper 1, when a total TRM is acquired by cooling from above the Curie temperature T_c to room temperature T_o in a field H_o, a wall is either thermally blocked at T_{Bf}, field blocked at T_B ($< T_{Bf}$ but $> T_o$), or reequilibrated at T_o, depending largely on the microcoercivity h_c encountered by the wall. Thermal blocking occurs only for walls with a small activation volume and a small H_o/h_{co} (h_{co} is h_c at T_o). The resulting T_{Bf} is very close to T_c. Walls with relatively large activation volumes are either field blocked or reequilibrated, and the corresponding TRM at T_o is given by

$$m_{tr}(T_o) = \frac{n h_{co}^{1/n} H_o^{1-1/n}}{(n-1)^{1-1/n} N} \qquad h_{co} \geq \frac{n^{n/(n-1)}}{n-1} H_o$$

$$m_{tr}(T_o) = \frac{h_{co}}{N} \qquad 0 \leq h_{co} < \frac{n^{n/(n-1)}}{n-1} H_o, \tag{3}$$

where N is the demagnetizing factor. The first alternative of (3) corresponds to field-blocked walls and has been calculated by a number of authors [*Néel*, 1955; *Everitt*, 1962; *Dunlop and Waddington*, 1975]; the second corresponds to reequilibrated walls. The boundary given in (3) that separates the field blocking and wall reequilibration regions represents the condition that the self-demagnetizing field $Nm_{tr}(T_o)$ must be smaller than the microcoercivity h_{co} in order for walls to remain field blocked at T_o when $H_o \to 0$; otherwise, walls reequilibrate. The field blocking temperature T_B is conveniently expressed in terms of $\beta(T_B) \equiv M_s(T_B)/M_s(T_o)$ and has been given by equation (10) in paper 1 as

$$\beta(T_B) = \left[\frac{H_o}{(n-1)h_{co}}\right]^{\frac{1}{n}}. \tag{4}$$

Thus a large H_o or a small h_{co} lowers T_B.

The total TRM intensity $M_{tr}(T_o)$ for an ensemble of MD grains with a distribution of microcoercivities $f(h_{co})$ is obtained by substituting (3) into (2), which gives

$$M_{tr}(T_o) = \frac{1}{N} \int_0^{n^{n/n-1}H_o^{1/(n-1)}} h_{co} f(h_{co})\, dh_{co} + \frac{n H_o^{1-1/n}}{(n-1)^{1-1/n} N} \int_{n^{n/n-1}H_o^{1/(n-1)}}^{\infty} h_{co}^{1/n} f(h_{co})\, dh_{co}. \tag{5}$$

The first integral in (5) represents the contribution from reequilibrated walls, and the second integral represents the contribution from field blocked walls. The upper limit $h_{co} \to \infty$ in the second integral in (5) has no physical reality, but it simplifies the calculation and gives no noticeable error (because of the use of an exponential distribution of $f(h_{co})$, as given in (1)).

Figure 1 shows the TRM induction curves (solid) calculated from (5) for $n = 2$ and $H_{co} = 1$, 2 and 5 mT. Figure 2 is for $n = 4$. The value of the demagnetizing factor N in (5) was taken to be 1/3 ($4\pi/3$ in cgs). In both figures, the slopes of the induction curves for small H_o values are close to $1 - 1/n$, indicating that the TRMs are predominantly field blocked (the second integral in (5)). When $H_o > H_{co}$, the M_{tr} values are predominantly determined by wall reequilibration (the first integral in (5)). The saturation value of $M_{tr}(T_o)$ is equal to the saturation remanence $M_{rs} = H_{co}/N$ as can be determined by integrating from zero to ∞ the first integral in (5).

For comparison, we also show in Figures 1 and 2 the results obtained using (3) for grains with a single value of microcoercivity (the dashed curves). The most noticeable modification by

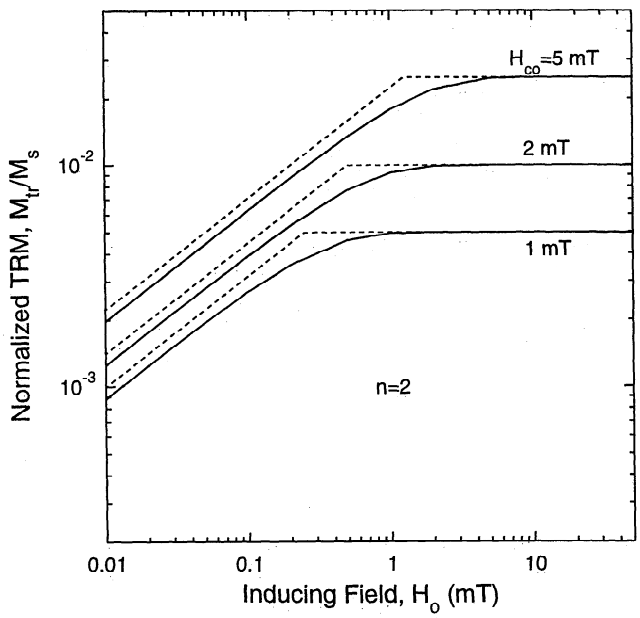

Fig. 1. The induction of total TRM as a function of inducing field H_o predicted by the theory, assuming that microcoercivity varies with temperature as $M_s^2(T)$ (i.e., $n = 2$). The solid curves are for grains having exponentially distributed microcoercivities, whose mean value at room temperature is H_{co}. The dashed curves are for grains with a single value ($= H_{co}$) of microcoercivity.

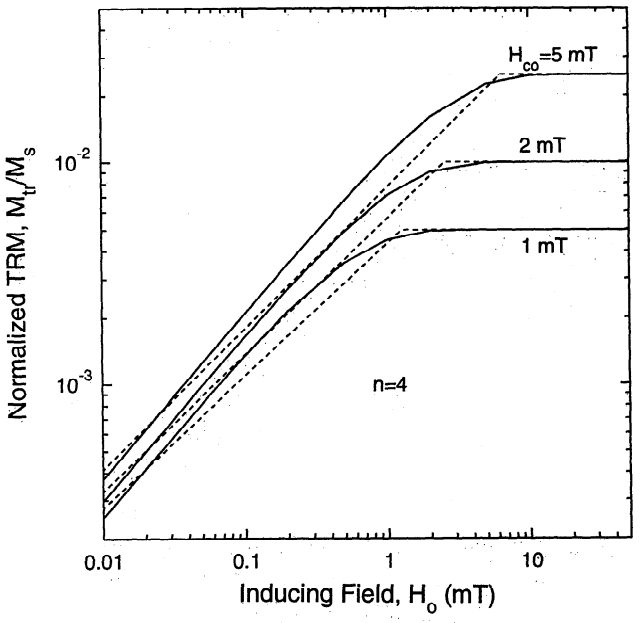

Fig. 2. The same as Figure 1 but assuming $n = 4$.

using a microcoercivity distribution is the smoothing of the transition from the field blocking-controlled to wall reequilibration-controlled M_{tr}.

For a given H_{co}, a larger value of n results in a smaller intensity of M_{tr} below saturation. This is largely because when n is larger, $h_c(T_B)$ is smaller (equation (4)) and consequently so is M_{tr} ($m_{tr} \propto h_c(T_B)$).

Figures 1 and 2 do not show a linearity between M_{tr} and H_o as observed when H_o is small. This is undoubtedly because we did not consider in (5) the contribution from thermally blocked walls. The thermally blocked TRM is linearly proportional to H_o (see paper 1 for a discussion of thermally blocked TRM).

The theory predicts a transition from field-blocked to wall reequilibrated TRM at $H_o \approx H_{co}$ (Figures 1 and 2). Experimentally, the transition is observed at a much higher H_o for MD grains (see Figure 6 of paper 1). The discrepancy is likely caused by the screening effect associated with the magnetostatic interaction among grains and/or among walls in individual grains [*Moon and Merrill*, 1986; *Xu and Merrill*, 1990*b*]. This effect cannot be calculated quantitatively with our two-domain model but may be intuitively seen as follows. With screening, the effective magnetic field H_{eff} (the sum of H_o and the demagnetizing field associated with magnetization of soft grains and/or displacement of soft walls) is only a fraction of H_o and may be written as $H_{eff} = \alpha H_o$ [*Xu and Dunlop*, 1993] ($\alpha \le 1$ is the screening factor and the equality holds when there is no screening). Consequently, the transition field observed should be $\approx H_{co}/\alpha$. For $\alpha \ll 1$ [*Moon and Merrill*, 1986; *Xu and Merrill*, 1990*b*; see also *Stacey and Banerjee*, 1974], we then have a transition field $\gg H_{co}$.

4. Thermal Demagnetization of Total TRM

During a zero-field heating to an elevated temperature T, the field-blocked walls will remain blocked if the microcoercivity $h_c(T)$ is larger than the self-demagnetizing field $Nm_{tr}(T)$ where m_{tr} is given by the first alternative in (3). This gives

$$h_c(T) > \frac{n^{n/(n-1)}}{n-1} H_o . \tag{6}$$

Otherwise, the walls will first unblock at T_B' ($< T$) and then continuously reequilibrate when heated above T_B'. Thus T_B' is the minimum unblocking temperature at which $h_c(T_B') = Nm_{tr}(T_B')$. From (6) we have

$$h_c(T_B') = h_{co}\beta^n(T_B') = \frac{n^{n/(n-1)}}{n-1} H_o . \tag{7}$$

Comparing (7) with (4) yields a relationship between the blocking temperature T_B and the minimum unblocking temperature T_B', given as

$$\beta(T_B') = n^{1/(n-1)}\beta(T_B) , \tag{8}$$

as obtained in paper 1 (equation (23)). Once the walls reequilibrate at T, the remanence is $h_c(T)/N$ when measured at T or $h_c(T)/\beta(T)N$ when measured at T_o. Consequently, the TRM remaining after a stepwise thermal demagnetization (i.e., the remanence measured at T_o) is

$$m_{tro}(T) = \frac{n h_{co}^{1/n} H_o^{1-1/n}}{(n-1)^{1-1/n} N} \qquad h_{co} \ge \frac{n^{n/(n-1)} H_o}{(n-1)\beta^n(T)}$$

$$m_{tro}(T) = \frac{h_{co}\beta^{n-1}(T)}{N} \qquad 0 \le h_{co} < \frac{n^{n/(n-1)} H_o}{(n-1)\beta^n(T)} . \tag{9}$$

The first alternative of (9) is for the walls that remain field blocked, and the second alternative is for the walls that reequilibrate at T. The boundary between the two is from (6). If it is a continuous thermal demagnetization (i.e., the remanence is measured at T), we have $m_{tr}(T) = \beta(T) m_{tro}(T)$. In (9) and below, we do not consider thermally blocked walls, for which the construction of a theory requires the distribution of activation volumes associated with Barkhausen jumps, which is unknown.

For an ensemble of grains, the TRM remaining is obtained by integrating (9) over the distribution of h_c values, giving

$$M_{tro}(T) = \frac{\beta^{n-1}(T)}{N} \int_0^{n^{n/(n-1)} H_o/[(n-1)\beta^n(T)]} h_{co}\, f(h_{co})\, dh_{co}$$

$$+ \frac{n H_o^{1-1/n}}{(n-1)^{1-1/n} N} \int_{n^{n/(n-1)} H_o/[(n-1)\beta^n(T)]}^{\infty} h_{co}^{1/n}\, f(h_{co})\, dh_{co} . \tag{10}$$

When $H_o \gg H_{co}$, we have $M_{tr} \to M_{rs}$. By setting the integral limit $n^{n/(n-1)}H_o/[(n-1)\beta^n(T)]$ in (10) to ∞, we obtain the saturation remanence M_{rso} remaining after demagnetizing at T:

$$M_{rso}(T) = \frac{\beta^{n-1}(T)H_{co}}{N}. \tag{11}$$

Thus $M_{rso}(T)$ follows $\beta^{n-1}(T)$ in a stepwise thermal demagnetization; in a continuous thermal demagnetization, $M_{rs}(T) \propto \beta^n(T)$.

We compare in Figure 3 the $M_{tro}(T)$ calculated from (10) with thermal demagnetization data of TRM measured by *Day* [1977] on a MD sample of titanomagnetite with $x = 0.6$ (TM60). In the calculation, H_{co} was taken to be equal to the bulk coercivity of 13.2 mT measured for the sample, $\beta(T) \propto (T - T_c)^{0.4}$ [*Moskowitz and Halgedahl*, 1987], and $T_c = 170°C$ as estimated from the data. The value of n for the sample is less certain, however. The slope of the TRM induction curve reported by *Day* [1977] for the sample gives $n = 2.86$. The theoretical curve calculated using this n value in (11) for saturation remanence actually fits the data quite well. However, using the same n value in (10) for the TRMs gives unblocking temperatures higher than measured and the discrepancy becomes larger when H_o is smaller. To give a reasonable fit, we used a varying value of n for different H_o values as indicated in Figure 3.

There are two possible causes for the varying value of n in Figure 3. The first is the fact that in deriving (10) we neglected thermally blocked walls, which are expected to play a more important role when a TRM is induced in a smaller H_o.

The varying value of n in Figure 3 may also be caused by the fact that different h_c fractions in the sample have different temperature dependences. A TRM induced in a small H_o will have a relatively large contribution from walls with small h_c values. Thus for the variation of n with H_o implied by Figure 3, we require smaller h_c values to vary relatively faster with T. Evidence supporting this is provided by *Tucker and O'Reilly* [1980], who showed that the temperature dependence of bulk coercivity for their TM60 samples can be generally fitted by a hard component varying slowly with T and a soft one varying relatively fast ($n \approx 7$). Their interpretation was that there exist two different types of defects controlling bulk coercivities of the TM60 samples. More discussion on this for magnetite samples will be given in section 7.

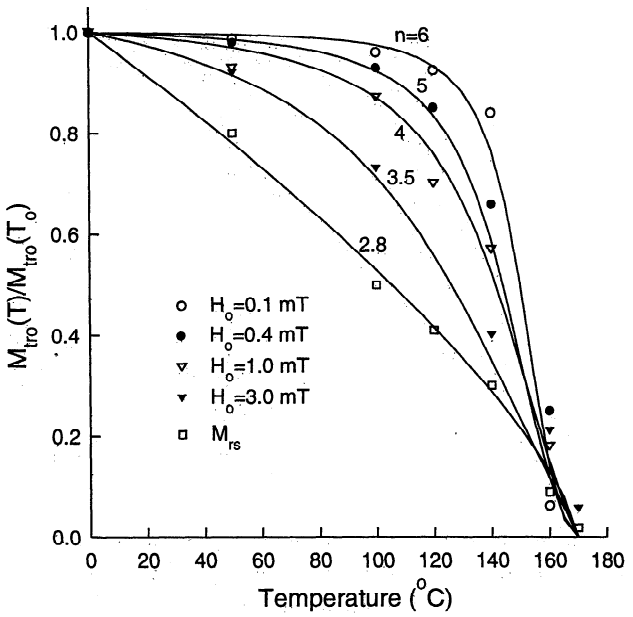

Fig. 3. Normalized thermal demagnetization curves of TRMs acquired in various fields H_o and of saturation remanence for MD grains of TM60 (grain size = 6.4 μm). The data points were measured by *Day* [1977]. The curves are the theoretical results calculated from (10) (for TRMs) and (11) (for saturation remanence) for the values of n indicated.

Both the theory and experiment indicate that a TRM induced in a large H_o has low unblocking temperatures. It is clear from (9) that for a given distribution of h_c values, a larger H_o will result in a TRM that has more reequilibrated walls and fewer field-blocked walls. Consequently, the TRM will have lower unblocking temperatures because the minimum unblocking temperature for the reequilibrated walls is T_o (i.e., they begin to unblock immediately when heated above T_o) while the minimum unblocking temperature for the field-blocked walls is $T_B' \geq T_o$ ((8) and (4)).

5. Some Differences Between Total TRM and Partial TRM

There are two types of partial TRMs: one is acquired from T_c to $T_1 \neq T_o$ and the other from $T_2 < T_c$. The treatment of the first type of partial TRM is in principle the same as a total TRM (see section 7 in paper 1) and thus it will not be considered in this and following sections. Henceforth "pTRM" will refer solely to the second type of partial TRM.

Differences between total TRM and pTRM can be traced to different initial wall positions: For a total TRM, walls start from some magnetized positions (determined largely by where they are nucleated), while for pTRM, walls start at a demagnetized state (for T_2 < a few degrees below T_c). When H_o is first turned on at T_2 for pTRM acquisition, walls are displaced to

$$\frac{m(T_2)}{M_s(T_2)} = \frac{H_o - h_c(T_2)}{M_s(T_2)N} \tag{12}$$

for $H_o > h_c(T_2)$ (cf. (28) in paper 1). At this stage of pTRM acquisition, h_c works against the wall displacement away from a demagnetized state as indicated by the minus sign in (12). As a comparison, h_c opposes any wall displacement toward a demagnetized state during TRM acquisition. This leads to two differences, as discussed below.

5.1. *Possible Lack of Field Blocking in pTRM Acquisition*

In order for a wall to be field-blocked in pTRM acquisition, it is necessary that the initial wall displacement given by (12) be larger than $m(T_B)/M_s(T_B)$ which is the field blocking position for TRM. This condition leads to inequality (32) in paper 1 and can be expressed as

$$\frac{H_o}{h_c(T_2)} \geq a_n \tag{13}$$

((34) in paper I). The a_n in (13) is the root of the following equation:

$$y - \frac{n}{(n-1)^{1-1/n}} y^{1-1/n} - 1 = 0 \tag{14}$$

((33) in paper 1). On the other hand, for a wall to remain field blocked when $H_o \to 0$ at T_1, T_1 must be lower than the minimum unblocking temperature T_B'. This is equivalent to requiring $h_c(T_1) > h_c(T_B')$. Using (7), this gives

$$\frac{H_o}{H_c(T_1)} < \frac{n-1}{n^{n/(n-1)}} \equiv b_n \tag{15}$$

((35) in paper 1). Using $h_c(T) = \beta^n(T)h_{co}$ and combining (13) and (15), we then obtain the necessary and sufficient condition for field blocking in pTRM, namely

$$\frac{\beta(T_1)}{\beta(T_2)} \geq \left[\frac{a_n}{b_n}\right]^{\frac{1}{n}} \tag{16}$$

which is independent of both H_o and h_c. The function of n given on the right-hand side of (16) decreases with increasing n. Thus for a given temperature interval (T_2, T_1), field blocking occurs more readily when n is larger, that is, when h_c changes faster with T. By taking $\beta(T) \propto (T_c - T)^{\gamma}$, where γ is a constant to be experimentally determined, and rearranging (16), we have

$$1 - \frac{T_2}{T_c} \geq (1 - \frac{T_1}{T_c})\left[\frac{b_n}{a_n}\right]^{\frac{1}{n\gamma}}, \tag{17}$$

where T_1, T_2, and T_c are in degrees Celsius. Field blocking is permitted in pTRM acquisition only when a chosen temperature interval (T_2, T_1) satisfies the inequality (17).

Plotted as lines in Figure 4 are the values of (T_2, T_1) given by the equality corresponding to (17) for n values ranging from 2 to 5. The value of γ is taken to be 0.43 as for magnetite [*Levi and Merrill*, 1978; *Worm et al.*, 1988; *Newell et al.*, 1990] (See also Figure 14 of paper 1]. Field blocking is forbidden if a chosen pair of (T_2, T_1) falls below the corresponding line for a given n, regardless of H_o and h_c. When n is larger (h_c changes faster with T), field blocking occurs over a broader (T_2, T_1) range.

As an example, consider a pTRM acquired from T_2 to room temperature (i.e., $T_1 = T_o$). We find that for magnetite there will be no field blocking if $T_2/T_c < 0.97$ or $T_2 < 565°C$ for $n = 2$ and $T_2/T_c < 0.85$ or $T_2 < \approx 500°C$ for $n = 4$. Comparing with total TRM acquisition, there will be no field-blocked walls if the minimum unblocking temperature T_B' is $> T_o$ (cf. section 4 of paper 1). Using (8), we then have $\beta(T_B) < n^{-1/(n-1)}$. Thus in total TRM acquisition, field blocking is not permitted at $T < T_B' \approx 465°C$ for $n = 2$ or $\approx 380°C$ for $n = 4$. (In paper I, we found $T_B' \approx 495°C$ for $n = 2$. This difference is due to the use of different $M_s(T)$ values; $M_s(T)$ was taken directly from measured data in paper 1 but here it is taken to be $\propto (T_c - T)^{0.43}$. The error thus introduced can be seen directly from the difference between the measured data and the theoretical curve for a given β in Figure 14, paper 1.)

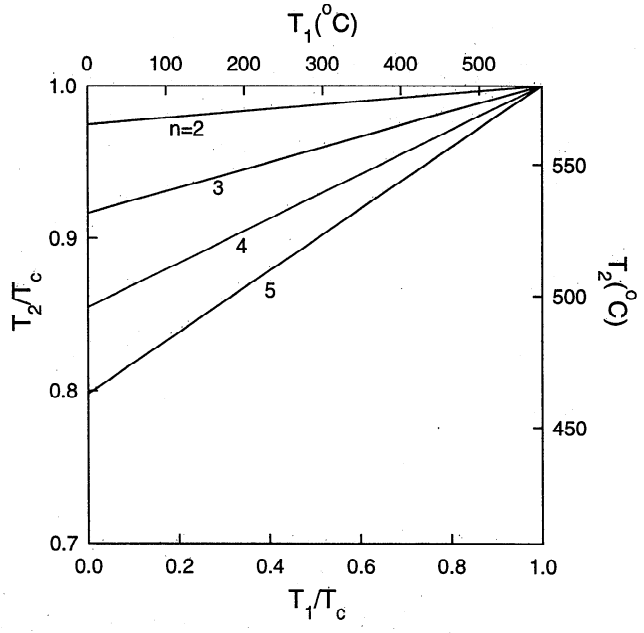

Fig. 4. Permitted and forbidden ranges for field blocking of pTRM. If a given (T_2, T_1) pair plots above the line for a particular value of n, field blocking is permitted. If (T_2, T_1) plots below the line, field blocking is forbidden and walls will either be isothermally blocked at T_2 or reequilibrate at T_1 (see also Table 3 of paper 1).

Clearly, the field-blocking range is much more restricted in partial TRM than in total TRM. We need a T_2 much higher than T_B in order to have field-blocked walls in pTRM acquisition. In the example given above, if $T_1 > T_o$, then an even higher T_2 is needed. *Worm et al.* [1988] used a temperature range of $(T_2, T_1) = (400, 350)°C$ in their pTRM experiment (these data will be used in section 7 for testing our pTRM theory). Figure 4 indicates that there will be no field-blocked walls in such a temperature range for any reasonable value of n.

5.2. *Isothermal Blocking*

This term refers to the blocking of walls that remain at their initial ($T = T_2$) positions, given by (14), when $H_o \to 0$ at T_1. This blocking process has no analog in total TRM acquisition but is similar to that in IRM (isothermal remanence) acquisition. The condition for a wall to be isothermally blocked is that the demagnetizing field at T_1 associated with the wall displacement given by (12) is smaller than $h_c(T_1)$. Using (12) and rearranging, we then have

$$\frac{H_o}{h_{co}} \leq \beta^n(T_2) + \beta(T_2)\beta^{n-1}(T_1). \tag{18}$$

A critical temperature $(T_1)_{crit}$ was defined in paper 1 when the equality sign holds in (18). If h_{co} of a wall satisfies inequality (18) (for given H_o and (T_2, T_1)), the wall will be isothermally blocked; otherwise, it will be either field blocked or reequilibrate when $H_o \to 0$ at T_1 (cf. equation (37) in paper 1).

6. Acquisition and Thermal Demagnetization of pTRM

The pTRM theory developed in this section will not include field-blocked walls, although it can be extended to deal with this situation. With no field blocking, when $H_o \to 0$ at T_1, walls either reequilibrate or are isothermally blocked. The boundary between the two is given by (18). The pTRM intensity for reequilibrated walls is given by the second alternative of (3) by replacing h_{co} by $h_c(T_1)$ and that for isothermally blocked walls is $m(T_2)/\beta(T_2)$ where $m(T_2)$ is given by (12). Thus the room temperature intensity of pTRM is

$$m_{ptr}(T_2, T_1, H_o) = 0 \quad \text{if} \quad h_{co} > \frac{H_o}{\beta^n(T_2)}$$

$$m_{ptr}(T_2, T_1, H_o) = \frac{H_o - h_{co}\beta^n(T_2)}{N\beta(T_2)}$$

$$\text{if} \quad \frac{H_o}{\beta^n(T_2) + \beta(T_2)\beta^{n-1}(T_1)} < h_{co} \leq \frac{H_o}{\beta^n(T_2)}$$

$$m_{ptr}(T_2, T_1, H_o) = \frac{h_{co}\beta^{n-1}(T_1)}{N}$$

$$\text{if} \quad h_{co} \leq \frac{H_o}{\beta^n(T_2) + \beta(T_2)\beta^{n-1}(T_1)} \tag{19}$$

(also see equation (36) in paper 1). The first alternative in (19) corresponds to trapped walls, the second to isothermally blocked walls and the third to reequilibrated walls. Averaging (19) over the microcoercivity distribution $f(h_{co})$, we obtain the room temperature intensity of the pTRM for an ensemble of grains, given as

$$M_{ptr}(T_2, T_1, H_o) = \frac{\beta^{n-1}(T_1)}{N} \int_0^{H_o/[\beta^n(T_2)+\beta(T_2)\beta^{n-1}(T_1)]} h_{co} f(h_{co}) dh_{co}$$

$$+ \frac{1}{N\beta(T_2)} \int_{H_o/[\beta^n(T_2)+\beta(T_2)\beta^{n-1}(T_1)]}^{H_o/\beta^n(T_2)} [H_o - h_{co}\beta^n(T_2)] f(h_{co}) dh_{co}. \quad (20)$$

The integral (20) can be carried out analytically for the microcoercivity distribution $f(h_{co})$ given by (1), and the resulting M_{ptr} is given in the appendix. We can also make an approximation for (20) by expanding $f(h_{co})$ in a Taylor's series and using only its first term (i.e., 1). The assumption in doing so is that the microcoercivities that are activated during a pTRM acquisition (i.e., represented by the integral limits of $0 < h_{co} \le H_o/\beta^n(T_2)$ in (20)) are such a small fraction that their distribution is approximately constant. This should be a good approximation for a pTRM acquired in a small H_o and from T_2 not close to T_c. Under this approximation, we have from (20)

$$M_{ptr}(T_2, T_1, H_o) \approx \frac{H_o^2}{2NH_{co}} \frac{\beta^{n-1}(T_1)}{\beta^{n+1}(T_2)[\beta^{n-1}(T_1) + \beta^{n-1}(T_2)]} \quad (21)$$

((21) can also be obtained by expanding the exponential terms in equation (28), as given in the appendix, into a Taylor's series to third order.) The resulting intensity of pTRM is proportional to the square of the inducing field H_o and inversely proportional to the mean microcoercivity H_{co}.

Consider now the thermal demagnetization of the pTRM given in (19). During a zero-field heating to T, the isothermally blocked walls will remain blocked if the demagnetizing field Nm_{ptr} of the walls is smaller than $h_c(T)$. Using (19) and rearranging, this gives

$$\frac{H_o}{h_{co}} \le \beta^n(T_2) + \beta(T_2)\beta^{n-1}(T) \quad (22)$$

Inequality (22) becomes (18) when T is replaced by T_1, as should be the case since the two inequalities represent a condition under which isothermally blocked walls will not reequilibrate at T_1 ((18)) or T ((22)) in zero field. The walls that do not satisfy condition (22) reequilibrate at T. Consequently, the pTRM remaining for both types of walls is (using (19) and (22))

$$m_{ptro}(T) = 0 \quad \text{if} \quad h_{co} \ge \frac{H_o}{\beta^n(T_2)}$$

$$m_{ptro}(T) = H_o - \frac{h_{co}\beta^n(T_2)}{N\beta(T_2)}$$

$$\text{if} \quad \frac{H_o}{\beta^n(T_2) + \beta(T_2)\beta^{n-1}(T)} < h_{co} \le \frac{H_o}{\beta^n(T_2)}$$

$$m_{ptro}(T) = \frac{h_{co}\beta^{n-1}(T)}{N}$$

$$\text{if} \quad h_{co} \le \frac{H_o}{\beta^n(T_2) + \beta(T_2)\beta^{n-1}(T)} \quad (23)$$

when measured at T_o (i.e. after a stepwise thermal demagnetization). Averaging (23) over the microcoercivity distribution $f(h_{co})$ yields the pTRM remaining for an ensemble of grains, given as

$$M_{ptro}(T) = \frac{\beta^{n-1}(T)}{N} \int_0^{H_o/[\beta^n(T_2)+\beta(T_2)\beta^{n-1}(T)]} h_{co} f(h_{co}) dh_{co}$$

$$+ \frac{1}{N\beta(T_2)} \int_{H_o/[\beta^n(T_2)+\beta(T_2)\beta^{n-1}(T)]}^{H_o/\beta^n(T_2)} [H_o - h_{co}\beta^n(T_2)] f(h_{co}) dh_{co} \quad (24)$$

for $T \ge T_1$; for $T < T_1$, there should be no change in the pTRM intensity. If the remanence is measured at T as in a continuous thermal demagnetization, the pTRM remaining is $M_{ptr}(T) = \beta(T)M_{ptro}(T)$.

The full analytical expression of $M_{ptro}(T)$ in (24) is given in the appendix. If we use the same approximation as used for obtaining (21), we obtain the simplified expression:

$$M_{ptro}(T) \approx \frac{H_o^2}{2NH_{co}} \frac{\beta^{n-1}(T)}{\beta^{n+1}(T_2)[\beta^{n-1}(T) + \beta^{n-1}(T_2)]} \quad (25)$$

for $T > T_1$.

From (21) and (25), the normalized pTRM as a function of demagnetizing temperature T is

$$\frac{M_{ptro}(T)}{M_{ptro}(T_o)} \approx \left[\frac{\beta(T)}{\beta(T_1)}\right]^{n-1} \frac{\beta^{n-1}(T_1) + \beta^{n-1}(T_2)}{\beta^{n-1}(T) + \beta^{n-1}(T_2)} \quad (26)$$

for a stepwise thermal demagnetization. For a continuous thermal demagnetization, we simply multiply (26) by $\beta(T)$. Thus to a first-order approximation, the normalized intensity of pTRM remaining is independent of both the inducing field H_o and the mean microcoercivity H_{co}. After demagnetizing at $T = T_2$, the pTRM remaining from (26) is

$$\frac{M_{ptro}(T_2)}{M_{ptro}(T_o)} \approx \frac{1}{2}\left[1 + \frac{\beta^{n-1}(T_2)}{\beta^{n-1}(T_1)}\right], \quad (27)$$

which is < 1 since $T_2 > T_1$. A complete demagnetization of pTRM occurs only when T reaches the thermal unblocking temperature T_{Bf} which is close to T_c (see the discussion of thermal blocking and unblocking in paper 1).

7. Comparison Between Theory and Experiment

Figure 5 shows the measured thermal demagnetization curves of pTRMs (dashed) for 35 μm magnetite grains from *Bolshakov and Shcherbakova* [1979]. The pTRMs were acquired in $H_o = 0.4$ mT in cooling from various T_2 values to room temperature. They were then continuously thermally demagnetized. All the pTRMs were completely thermally demagnetized only when heated to $T \simeq T_c$, as predicted by the theory given in last section. The solid curves were calculated using (25) multiplied by $\beta(T)$ (and also by an arbitrary constant because of unknown factors such as the total volume of magnetite grains in the sample), with $M_s(T) \propto (T_c - T)^{0.43}$. The value of n used in (25) was 3 for $T_2 = 400$°C and 4 for $T_2 = 300$ and 200°C, chosen so as to give a good fit to the data. The fact that these demagnetization curves cannot be fitted using the same value of n is likely due to the same reasons discussed in section 4 for the thermal demagnetization of total TRM; namely, (1) neglect in our model of thermally blocked walls whose contribution to pTRM is expected to be increasingly important with increasing T_2 and (2) existence of different types of defects in the sample, resulting in h_c fractions having different temperature dependences.

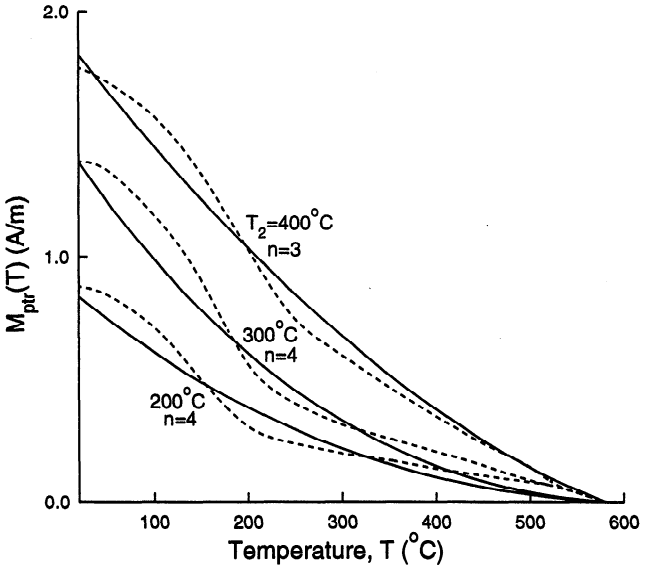

Fig. 5. Continuous thermal demagnetization curves (dashed) of pTRMs for 35 μm magnetite grains from *Bolshakov and Shcherbakova* [1979]. The pTRMs were acquired in a 0.4 mT field by cooling from the different T_2 values indicated to room temperature. The solid curves are the theoretical results calculated from (25) multiplied by $\beta(T)$.

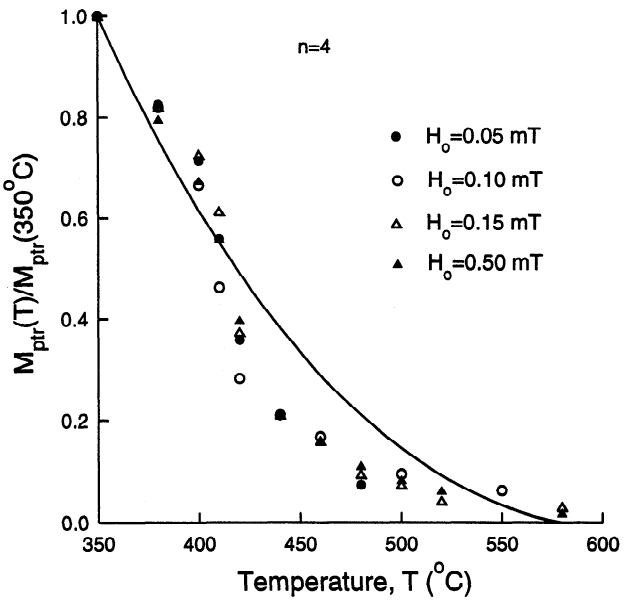

Fig. 6. Continuous thermal demagnetization data of pTRMs acquired in the range (400°, 350°C) in different inducing fields for 3 μm magnetite grains from *Worm et al.* [1988]. A rather sharp drop at 400°C is apparently associated with thermal unblocking of some single-domain component. When normalized, the thermal demagnetization of the pTRMs is independent of the inducing field H_o, as predicted by the theory (equation (26)) and shown by the solid curve.

Figure 6 shows the pTRM data for 3 μm magnetite grains from *Worm et al.* [1988]. All the pTRMs were acquired in the same temperature interval (400°, 350°C), but in different fields H_o. According to Figure 4, there should be no field-blocked walls for a pTRM acquired in this temperature range. The pTRMs were then continuously thermally demagnetized and were completely demagnetized at $T \simeq T_c$ as in Figure 5. The solid curve is calculated using (26) with $n = 4$, and it provides an approximate fit to the data. One obvious reason for the misfit is that there is a certain amount of contribution from thermal blocking to the pTRMs, which is evidenced by a rather sharp drop of the pTRMs at about $T_2 = 400$°C. The thermal blocking in this case is likely associated with some single-domain component, considering the fact that the grains are in the pseudo-single-domain size range of magnetite.

Figure 7 shows the pTRM data for another sample from *Worm et al.* [1988]. They are for 40 μm magnetite grains and were acquired in the same temperature interval as used in Figure 6. The pTRMs in this case do not show a sharp decrease at 400°C. Instead, they vary quite smoothly with temperature, indicating a diminishing contribution from thermal blocking with increasing grain size. The solid curve is the same temperature dependence as used in Figure 6, and it gives a good fit to the pTRM induced in a 0.1 mT field. The misfit to the other two sets of pTRM data can be attributed partially to the noticeable scattering of the data.

For both the magnetite samples shown in Figures 6 and 7, the normalized pTRM thermal demagnetization curves are in first-order approximation independent of the inducing field H_o, as predicted by the theory (equation (25)). Moreover, the use of the same theoretical curve in Figures 6 and 7 for the two samples, which must have different H_{co} values, indicates that normalized pTRM thermal demagnetization curves are in first-order approximation independent of H_{co}, as predicted also by the theory (equation (25)).

The value of $n = 4$ used for the theoretical curves in Figures 6 and 7 is not compatible with the thermal variation of bulk coercivity $\propto M_s^{1.7}(T)$ reported by *Worm et al.* [1988]. The difference in n in this case is unlikely to be caused by neglect in

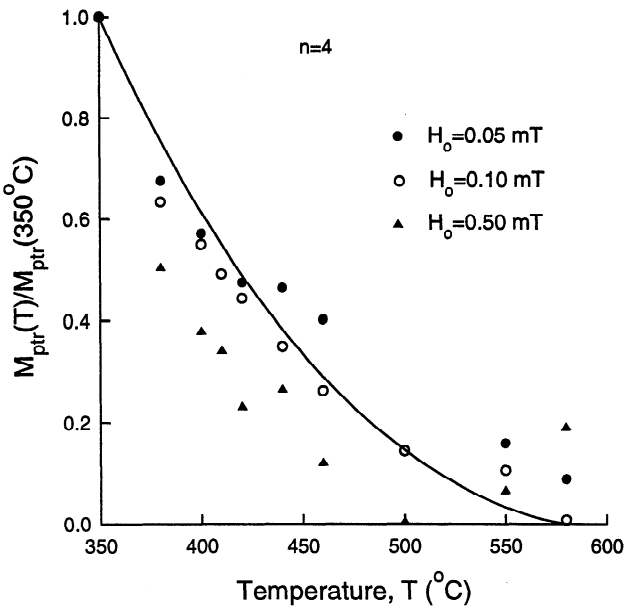

Fig. 7. Same as Figure 6 but for 40-μm grains. With an increase in grain size, the contribution from thermal blocking of single-domain pTRM diminishes, and the fit between the theory and experiment also improves (except for the 0.5-mT data which are anomalous at $T > 500$°C).

our model of thermal blocking, as its contribution has decreased with an increasing grain size from 3 μm to 40 μm. Instead, we suggest that this difference is caused by existence in the samples of different types of defects for which h_c values have different temperature dependences. Bulk coercivity measurements activate the entire h_c spectrum, whereas the (400°, 350°C) pTRMs activate only a part of the spectrum with relatively small h_c values. This leads to different n values between bulk coercivity and pTRM measurements.

8. DISCUSSION AND CONCLUSION

There are three different blocking processes during the acquisition of a total TRM: thermal blocking, field blocking and wall reequilibration. Thermal blocking is associated with walls with small activation volumes, whereas field blocking and wall reequilibration are associated with walls with relatively large activation volumes having large and small microcoercivities, respectively. The TRM intensity is linearly proportional to the inducing field H_o for thermal blocking, varies as $H_o^{1-1/n}$ for field blocking, and is independent of H_o for wall reequilibration. For an ensemble of grains with exponentially distributed microcoercivities, the intensity of TRM for a given H_o is predominantly governed by one of the three blocking processes, resulting in a TRM induction curve consisting of three distinctive H_o dependences (Figures 1 and 2).

Our theory predicts that the transition from the field blocking to wall reequilibration regime in a TRM induction curve occurs at $H_o \approx H_{co}$ (Figures 1 and 2). When $H_o > H_{co}$, M_{tr} approaches the saturation remanence M_{rs}. The observed transition field is often much larger than a sample's bulk coercivity, however. We suggest that this discrepancy is caused by magnetic screening by soft walls/grains, which is not considered in our present model. With screening, the effective field inside a grain is a factor α smaller than H_o [*Xu and Dunlop*, 1993] and consequently, the transition field is a factor α larger than the bulk coercivity.

During thermal demagnetization of TRM, reequilibrated walls will begin to unblock immediately above T_o, while field-blocked walls will begin to unblock at some $T_B' > T_o$. From (7), this T_B' is higher when the H_o/h_{co} ratio is smaller; that is, a field-blocked wall with a relatively high h_{co} will begin to unblock at a higher T. Thus if a TRM is predominantly carried by reequilibrated walls, as it will be if acquired in a high H_o, it will have low unblocking temperatures. This is evident both from the theory and from experiment, as shown in Figure 3. (This result is in contrast with the Lower-Fuller test, in which multidomain TRM induced in a higher H_o is harder to AF demagnetize.)

For a partial TRM, the field response depends additionally on the temperature range (T_2, T_1) $(T_2 \neq T_c)$ in which the pTRM is acquired. If the interval (T_2, T_1) is not large enough, there will be a complete lack of field-blocked walls. For magnetite, any pTRM acquired from $T_2 < 565°C$ to T_o will have no field-blocked walls if $n = 2$ (i.e., $h_c(T) \propto M_s^2(T)$) or from $T_2 < 500°C$ if $n = 4$ (Figure 4).

If there is no field blocking, walls either are isothermally blocked at T_2 or reequilibrate at T_1 when $H_o \to 0$. The isothermally blocked walls are those that are displaced by H_o at T_2 and then remain at the displaced positions throughout the subsequent cooling. Isothermally blocked walls and reequilibrated walls are always present in a pTRM; the former are associated with relatively large h_{co} values and the latter with small h_{co} values. In a first-order approximation, the pTRM intensity is predicted to be proportional to the square of H_o (when H_o is small and T_2 is not close to T_c).

When thermally demagnetized, the reequilibrated walls begin to unblock first, followed by the isothermally blocked walls with relatively low h_{co} values. The pTRM is completely demagnetized only at a thermal unblocking temperature T_{Bf} which is close to T_c. Our theory shows that in a first-order approximation, the pTRM remaining, normalized to the intensity before heating, is independent of both the inducing field H_o and the mean microcoercivity H_{co} (equation (25)), a prediction that is supported by the experimental data of *Worm et al.* [1988] (Figures 6 and 7).

Our theory implies that pTRMs for MD grains are neither additive nor independent, in contrast to SD grains. One obvious reason that pTRMs are not additive is that different blocking processes may be involved in different pTRMs, depending on the temperature interval in which each pTRM is acquired. For example, consider a pTRM acquired in (T_2, T_1) that contains field-blocked, isothermally blocked, and reequilibrated walls. When (T_2, T_1) is subdivided into smaller temperature intervals and in each a separate pTRM is acquired in the same H_o, these sub-pTRMs may completely lack field-blocked walls (see Figure 4). Thus there is no reason why the sum of these sub-pTRMs should be equal to the pTRM acquired in (T_2, T_1). (Also, see numerical examples given in Table 2 of paper 1.)

The independence of pTRMs is also not valid for MD grains, as any pTRM acquired in any temperature range whatever will be completely demagnetized only at a temperature close to T_c (Figures 5, 6, and 7).

The additivity and independence of pTRMs are two basic requirements for carrying out a successful determination of paleomagnetic field intensity, as pioneered by *Thellier* [1938]. The above discussion implies that MD grains are not suitable for determination of paleomagnetic field intensity, and in fact a nonlinear behaviour of MD samples treated by Thellier's method has been reported by *Levi* [1975, 1977]. Another potential failure of Thellier's method is that MD pTRMs are not linearly proportional to the inducing field H_o, according to (21). The proportionality between pTRM intensity and H_o is another basic requirement for the success of Thellier's method. In a future paper, we will give a detailed discussion of implications of our MD pTRM theory for the determination of paleomagnetic field intensity.

The fact that any pTRM is completely thermally demagnetized only at T close to T_c also implies that any pTRM acquired by MD grains in rocks as a secondary component will overlap and obscure the direction of a primary single-domain component right up to T_c in thermal cleaning. For a MD pTRM, AF cleaning should be more effective than thermal cleaning [cf. Schmidt, 1993]. This can be seen by noting that a pTRM should be AF demagnetized at a peak field approximately equal to the maximum h_{co} activated during pTRM acquisition. According to equation (19), $(h_{co})_{max} = H_o/\beta^n(T_2)$, which is not a large field for $H_o \approx$ the intensity of the Earth's magnetic field and T_2 not too high. For example, taking $H_o = 0.1$ mT and $T_2 < 500°C$ for magnetite, we have $(h_{co})_{max} < 1.3$ mT for $n = 2$ and < 3 mT for $n = 4$.

APPENDIX: ANALYTIC RESULTS FOR THE INTENSITY AND THERMAL DEMAGNETIZATION OF pTRM

Using (1) and carrying out the integration in (20), we obtain the intensity of pTRM (measured at T_o) acquired in a field H_o and in a temperature range (T_2, T_1) $(T_2 < T_c)$. This is

$$M_{ptr}(T_2, T_1) = \frac{\beta^{n-1}(T_1)H_{co}}{N} + \frac{\beta^{n-1}(T_2)H_{co}}{N}\exp\left[-\frac{H_o}{H_{co}\beta^n(T_2)}\right] - \frac{H_{co}}{N}[\beta^{n-1}(T_1) + \beta^{n-1}(T_2)]\exp\left[-\frac{H_o}{H_{co}\beta(T_2)[\beta^{n-1}(T_1) + \beta^{n-1}(T_2)]}\right], \quad (28)$$

where H_{co} is the mean microcoercivity. Correspondingly, the pTRM remaining after a stepwise thermal demagnetization at T is (from (24))

$$M_{\text{ptro}}(T) = \frac{\beta^{n-1}(T)H_{co}}{N}$$

$$+ \frac{\beta^{n-1}(T_2)H_{co}}{N}\exp\left[-\frac{H_o}{H_{co}\beta^n(T_2)}\right] - \frac{H_{co}}{N}[\beta^{n-1}(T)$$

$$+ \beta^{n-1}(T_2)]\exp\left[-\frac{H_o}{H_{co}\beta(T_2)[\beta^{n-1}(T) + \beta^{n-1}(T_2)]}\right]. \quad (29)$$

Acknowledgments. This research has been supported by the Natural Sciences and Engineering Research Council of Canada through operating grant A7709. Helpful reviews by Wyn Williams and Susan Halgedahl were much appreciated.

REFERENCES

Bailey, M.E., and D.J. Dunlop, Alternating field characteristics of pseudo-single-domain (2-14 μm) and multidomain magnetite, *Earth Planet. Sci. Lett., 63,* 335-352, 1983.

Bolshakov, A.S., and V.V. Shcherbakova, Thermomagnetic criteria for ferrimagnetic domain structure, *Izv. Akad. Nauk SSSR, Ser. Fiz. Zemli, 2,* 38-47, 1979.

Day, R., TRM and its variation with grain size, *J. Geomagn. Geoelectr., 29,* 233-265, 1977.

Dunlop, D.J., Determination of domain structure in igneous rocks by alternating field and other methods, *Earth Planet. Sci. Lett., 63,* 353-367, 1983.

Dunlop, D.J., and E.D. Waddington, The field dependence of thermoremanent magnetization in igneous rocks, *Earth Planet. Sci. Lett., 25,* 11-25, 1975.

Dunlop, D.J., and S. Xu, Theory of partial thermoremanent magnetization in multidomain grains, 1, Repeated identical barriers to wall motion (single microcoercivity), *J. Geophys. Res.,* this issue.

Everitt, C.W.F., Thermoremanent magnetization, III, Theory of multi-domain grains, *Philos. Mag., 7,* 599-616, 1962.

Levi, S., Comparison of two methods of performing the Thellier experiment (or, how the Thellier experiment should not be done), *J. Geomagn. Geoelectr., 27,* 245-255, 1975.

Levi, S., The effect of magnetite particle size on paleointensity determinations of the geomagnetic field, *Phys. Earth Planet. Inter., 13,* 245-259, 1977.

Levi, S., and R.T. Merrill, Properties of single-domain, pseudo-single-domain, and multidomain magnetite, *J. Geophys. Res., 83,* 309-323, 1978.

Moon, T., and R.T. Merrill, Magnetic screening in multidomain material, *J. Geomagn. Geoelectr., 38,* 883-894, 1986.

Moskowitz, B.M., and S.L. Halgedahl, Theoretical temperature and grain-size dependence of domain state in x=0.6 titanomagnetite, *J. Geophys. Res., 92,* 10,667-10,682, 1987.

Néel, L., Some theoretical aspects of rock magnetism, *Adv. Phys., 4,* 191-242, 1955.

Newell, A.J., D.J. Dunlop, and R.J. Enkin, Temperature dependence of critical sizes, wall widths and moments in two-domain magnetite grains, *Phys. Earth Planet. Inter., 65,* 165-176, 1990.

Schmidt, P.W., Paleomagnetic cleaning strategies, *Phys. Earth Planet. Inter., 76,* 169-178, 1993.

Schmidt, V.A., A multidomain model of thermoremanence, *Earth Planet. Sci. Lett., 20,* 440-446, 1973.

Stacey, F.D., Thermo-remanent magnetization (TRM) of multidomain grains in igneous rocks, *Philos. Mag., 3,* 1391-1401, 1958.

Stacey, F.D., and S.K. Banerjee, *The Physical Principles of Rock Magnetism,* 195 pp., Elsevier, New York, 1974.

Thellier, E., Sur l'aimantation des terres cuites et ses application géophysiques, *Ann. Inst. Phys. Globe Univ. Paris, 16,* 157-302, 1938.

Tucker, P., and W. O'Reilly, The acquisition of thermoremanent magnetization by multidomain single-crystal titanomagnetite, *Geophys. J. R. Astron. Soc., 60,* 2-36, 1980.

Worm, H-U., M. Jackson, P. Kelso, and S.K. Banerjee, Thermal demagnetization of partial thermoremanent magnetization, *J. Geophys. Res., 93,* 12,196-12,204, 1988.

Xu, S., and D.J. Dunlop, Theory of alternating field demagnetization of multidomain grains and implications for the origin of pseudo-single-domain remanence, *J. Geophys. Res., 98,* 4183-4190, 1993.

Xu, S., and R.T. Merrill, Microstress and microcoercivity in multidomain grains, *J. Geophys. Res., 94,* 10,627-10,636, 1989.

Xu, S., and R.T. Merrill, Microcoercivity, bulk coercivity and saturation remanence in multidomain materials, *J. Geophys. Res., 95,* 7083-7090, 1990*a*.

Xu, S., and R.T. Merrill, Toward a better understanding of magnetic screening in multidomain grains, *J. Geomagn. Geoelectr., 42,* 637-652, 1990*b*.

D. J. Dunlop and S. Xu, Geophysics Laboratory, Department of Physics, University of Toronto, Erindale Campus, Mississauga, Ontario, Canada L5L 1C6.

(Received December 10, 1992; revised August 30, 1993;
accepted September 8, 1993.)